

Richard W. Laton (S'65-M'71) was born in Springfield, IL. He received the B.S. degree from the U.S. Naval Academy and the M.S.E. and Ph.D. degrees in electrical engineering from the University of Michigan, Ann Arbor. The topic of his Ph.D. dissertation, completed in 1972, was "Characteristics of IMPATT Diode Reflection Amplifiers."

He was employed as a staff member at the M.I.T. Lincoln Laboratory, Lexington, MA, from 1972 to 1979, engaged in research and development of solid-state microwave devices and their application to phased-array radars. Since December of 1979, he has been with Raytheon's Missile Systems Division Bedford Laboratories where he has served as section manager for solid-state missile microwave transmitters as well as

for microwave sources and devices. His current position is that of program manager, Ballistic Intercept Missile.



J. Bradford Cole (S'81-M'84) was born in Pittsburgh, PA, in 1960. He received the B.S.E.E. degree from Carnegie-Mellon University, Pittsburgh, PA, in 1982, and the M.S.E.E. degree from the University of Massachusetts, Amherst, in 1984 on a Raytheon Fellowship.

Since 1982, he has been employed by Raytheon Company, Bedford, MA, where he has worked on low-noise oscillator design and multi octave monolithic amplifier design.

RF Spectrum of Thermal Noise and Frequency Stability of a Microwave Cavity-Oscillator

BERNARD VILLENEUVE, STUDENT MEMBER, IEEE, PIERRE TREMBLAY, STUDENT MEMBER, IEEE,
ALAIN MICHAUD, STUDENT MEMBER, IEEE, AND MICHEL TÉTU, SENIOR MEMBER, IEEE

Abstract — The spectral distribution of the thermal noise within a microwave cavity equipped with an external feedback loop has been calculated and measured. An equivalent electrical model is established from which the noise spectral density can be calculated at any port in the system. The effect of the gain and phase of the loop on the spectral distribution is measured with a spectrum analyzer through a heterodyne technique and comparison with theoretical calculations shows good agreement. Also, the modified cavity Q and resonant frequency is measured for various loop parameters. An experimental setup allowing precise measurement of frequency stability and FM noise close to carrier of microwave oscillators is presented and discussed. Preliminary measurements of the short-term frequency stability of the system when operated as a microwave cavity-oscillator show a predominant flicker frequency noise. The measured FM noise close to carrier is related to time-domain measurements of frequency stability and to RF spectrum of the cavity-oscillator.

I. INTRODUCTION

THE QUALITY FACTOR of a microwave cavity can be varied easily over a wide range if it is equipped with an external feedback loop having a variable gain and a variable total phase shift [1]. The Q factor can be reduced or increased, and the system becomes an oscillator when its value reaches infinity. Microwave cavities using such an artificially enhanced Q factor are encountered in

atomic frequency standard technology where small size devices are built using this approach [2]. With this type of standards, it has been observed through frequency stability measurements that the effect of thermal noise within the cavity varies greatly with the parameters of the external loop [3]. We present in this paper a theoretical evaluation of the spectral distribution of this thermal noise for various operating conditions and compare the calculated results to measured data. We give also preliminary results on the study of frequency stability and FM noise for this type of system when operated as a cavity-oscillator.

II. THERMAL NOISE

A. Radio-Electrical Model

The microwave cavity and its feedback loop (or the microwave cavity-oscillator) can be represented schematically through Fig. 1. Power is coupled in and out of the cavity with coupling coefficients β_2 and β_1 , respectively. The external loop consists of a low-noise GaAs FET amplifier, a variable attenuator, a variable phase shifter, and two isolators, one at each end of the loop. The output signal is observed through an AM heterodyne receiver. In this setup, discrete elements are used in order to evaluate separately their contribution to the behavior of the whole system.

Manuscript received May 7, 1984.

The authors are with Laboratoire de recherche sur les oscillateurs et systèmes, Département de génie électrique, Université Laval, Québec, G1K 7P4, Canada.

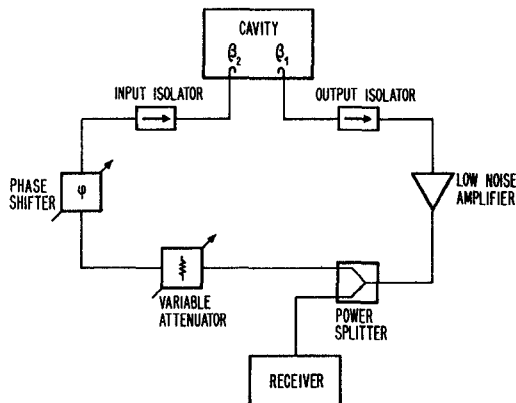


Fig. 1. Schematic diagram of a microwave cavity equipped with an external feedback loop.

An electrical circuit equivalent to the cavity and its loop is given in Fig. 2. We consider in this relatively simple model only the noise sources E_c from the cavity (black body radiation), E_1 and E_2 from the dummy loads of the isolators, E_a from the low-noise amplifier, and E_r from the receiver. The ψ_i 's represent the phase shifts between the loop elements at frequency f_0 , and the other symbols have the usual meanings.

In order to find an expression for the power spectral density of the voltage delivered to the load, we first evaluate the transfer functions for each independent noise source. Taking into account that $I_1 = n_1 I_c$, $I_2 = n_2 I_c$, $\beta_1 = n_1^2 Z_0 / R_c$, and $\beta_2 = n_2^2 Z_0 / R_c$ with Z_0 the transmission line characteristic impedance, it is relatively easy to show that the noise current I_c flowing in the cavity is given by

$$S_{V_0}(f) = \frac{1}{4} G_r^2 S_{E_r}(f) + \left\{ \frac{G_r^2 G_s^2 G_a^2}{(1 + \beta_1 + \beta_2 - 2G\sqrt{\beta_1\beta_2} \cos \psi)^2 + (Q_0\Delta - 2G\sqrt{\beta_1\beta_2} \sin \psi)^2} \right. \\ \left. \cdot \left\{ \frac{1}{4} [(1 + \beta_1 + \beta_2)^2 + (Q_0\Delta)^2] S_{E_c}(f) + \left(\frac{n_1 Z_0}{R_c} \right)^2 [n_1^2 S_{E_1}(f) + S_{E_c}(f) + n_2^2 S_{E_2}(f)] \right\} \right\}. \quad (5)$$

$$I_c = \frac{E_c - n_1 E_1 e^{-i\psi_1} - n_2 E_2 e^{i\psi_2} + n_2 G E_a e^{i(\psi_3 + \psi_4 + \psi_5 + \psi_6 + \psi_7 + \psi_8)}}{R_c (1 + \beta_1 + \beta_2 + iQ_0\Delta - 2G\sqrt{\beta_1\beta_2} e^{i\psi})} \quad (1)$$

where Q_0 is the unloaded cavity Q , G is the total loop voltage gain, and ψ is the total loop phase shift, which are

$$G = G_a G_s G_l \quad \text{and} \quad \psi = \sum_{i=1}^7 \psi_i + \psi_p \quad (2)$$

and Δ is defined as

$$\Delta = \frac{f}{f_0} - \frac{f_0}{f} \quad (3)$$

with f_0 the resonant frequency of the cavity.

The voltage V_0 delivered to the load is evaluated through the relation $V_0 = G_r V_r e^{i\psi_8}$, where G_r is the voltage conversion gain of the receiver and V_r its input voltage. A simple

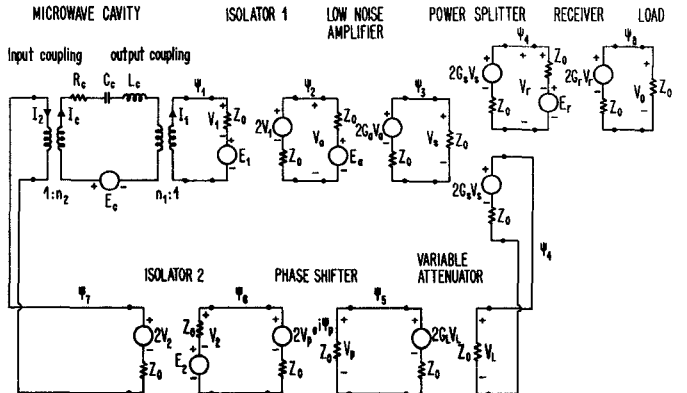


Fig. 2. Equivalent model of the cavity and its feedback loop.

calculation of V_0 gives

$$V_0 = \frac{1}{2} G_r E_r e^{i\psi_8} + \frac{G_r G_s G_a}{1 + \beta_1 + \beta_2 + iQ_0\Delta - 2G\sqrt{\beta_1\beta_2} e^{i\psi}} \\ \cdot \left[\frac{1}{2} (1 + \beta_1 + \beta_2 + iQ_0\Delta) E_a e^{i(\psi_3 + \psi_4 + \psi_8)} \right. \\ \left. + \frac{n_1 Z_0}{R_c} (-n_1 E_1 e^{-i\psi_1} + E_c - n_2 E_2 e^{i\psi_2}) \right. \\ \left. \cdot e^{(\psi_1 + \psi_2 + \psi_3 + \psi_4 + \psi_8)} \right]. \quad (4)$$

When the sources are independent random functions with spectral densities $S_{E_r}(f)$, $S_{E_a}(f)$, $S_{E_1}(f)$, $S_{E_2}(f)$, and $S_{E_c}(f)$, respectively, we find that the spectral density of the output voltage $S_{V_0}(f)$ is

The measured power spectral density delivered to the load $S_0(f)$ is equal to

$$S_0(f) = \frac{S_{V_0}(f)}{Z_0}. \quad (6)$$

Assuming we are dealing with thermal noise sources such that

$$S_{E_r}(f) = 4kZ_0T_r \quad S_{E_a}(f) = 4kZ_0T_a \quad S_{E_1}(f) = 4kZ_0\theta_1 \\ S_{E_2}(f) = 4kZ_0\theta_2 \quad \text{and} \quad S_{E_c}(f) = 4kR_c\theta_c$$

where T_r and T_a are the equivalent noise temperature of the receiver and the low-noise amplifier, respectively, while θ_1 , θ_2 , and θ_c are the thermodynamic temperatures of the isolators 1, 2, and the cavity, the complete calculation of $S_0(f)$ gives

$$S_0(f) = kG_r^2 G_a^2 G_s^2 \left\{ \frac{T_r}{G_a^2 G_s^2} + \frac{[(1 + \beta_1 + \beta_2)^2 + (Q_0\Delta)^2] T_a + 4\beta_1(\theta_c + \beta_1\theta_1 + \beta_2\theta_2)}{(1 + \beta_1 + \beta_2 - 2G\sqrt{\beta_1\beta_2} \cos \psi)^2 + (Q_0\Delta - 2G\sqrt{\beta_1\beta_2} \sin \psi)^2} \right\}. \quad (7)$$

Equation (7) gives the spectral distribution of the noise at the output of a receiver "looking" at a system "cavity + feedback loop." The first term is the contribution from the receiver while the second term represents the contribution of the noisy elements within the loop. This relation shows the fundamental process by which the spectral distribution of the thermal noise is modified.

Analyzing (4), we see that the feedback loop also modifies the quality factor and resonant frequency of the system operated as a transmission element (e.g., by injecting power with a directional coupler just after the phase shifter; see Fig. 1). The real part of the denominator in (1) is related to the Q which becomes, in terms of the loop gain G and the total loop phase shift ψ

$$Q = \frac{Q_0}{1 + \beta_1 + \beta_2 - 2G\sqrt{\beta_1\beta_2} \cos \psi}. \quad (8)$$

From the imaginary part of the same denominator, we obtain an expression for the system resonant frequency

$$f'_0 = f_0 \left(1 + \frac{G\sqrt{\beta_1\beta_2}}{Q_0} \sin \psi \right). \quad (9)$$

In the following sections we shall show the validity of (7)–(9).

B. Experimental Measurements

The power spectral distribution of the thermal noise generated within the system for various total loop gains and phase shifts is measured directly with a spectrum analyzer (AIL 757) at the IF frequency (30 MHz) of a low-noise heterodyne AM receiver. The loop gain G and the loop phase shift ψ are manually changed through the use of a micrometer variable attenuator (setting a) and a phase shifter (setting p). Calibration of the indicator settings is done by replacing the cavity by a network analyzer (HP8410), and measuring the gain and phase from the input of isolator 1 to the output of isolator 2. However, the measurements must be done at a relatively high power level and the loop amplifier begins to saturate, affecting loop gain and phase. A power meter is therefore used in place of the receiver (see Fig. 1) and its reading P_0 is chosen as a third loop parameter. During the calibrations, this power was monitored and maintained at $P_0 = 4.0$ dBm, a practical value. Fig. 3(a) and (b) gives the resulting variations of the loop gain and phase for the two parameters a and p , respectively. It is observed that the settings of these parameters do not provide independent control over the gain and phase. Fig. 3(c) gives the total gain and phase of the loop as functions of the output power P_0 , which allows their estimation at usual power levels (noise level). By proper use of Fig. 3(a)–(c) one can determine accurately the loop gain G and loop phase ψ for any parameter settings (a , p , and P_0).

Fig. 4(a) gives the noise-power spectral density for various attenuator settings (loop gain) while the phase shifter setting was maintained at a fixed value (total phase shift close to zero). It is observed that the curves are almost

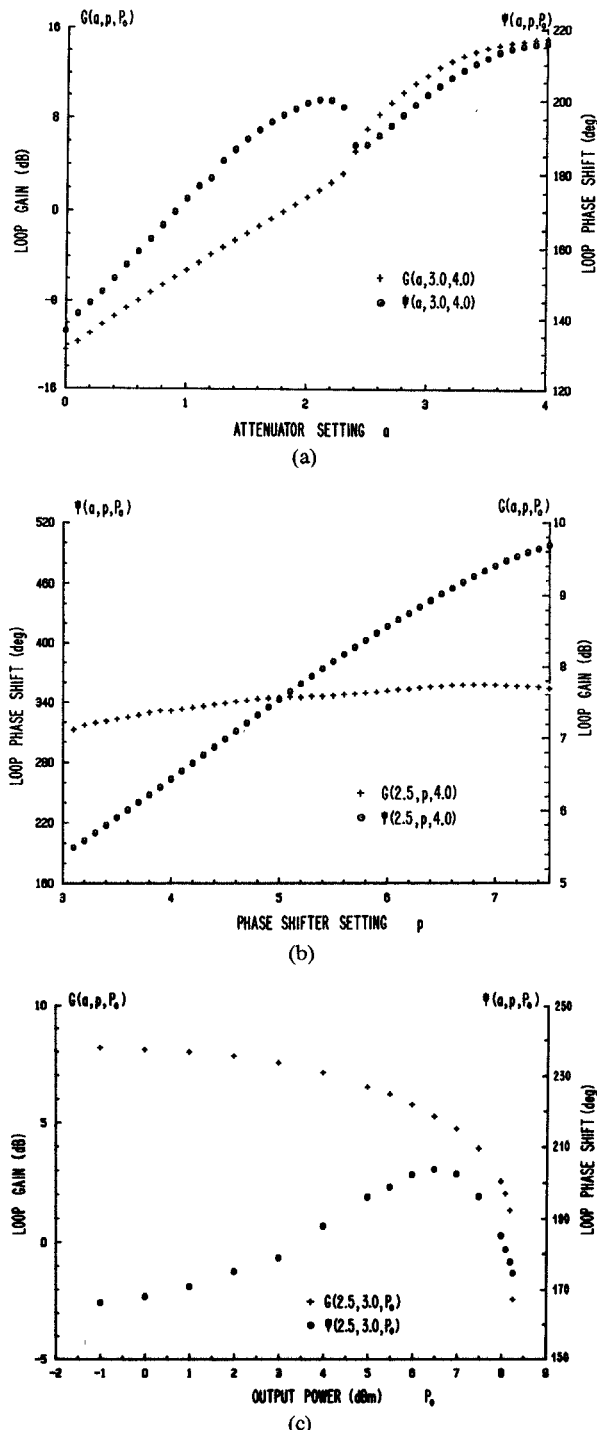
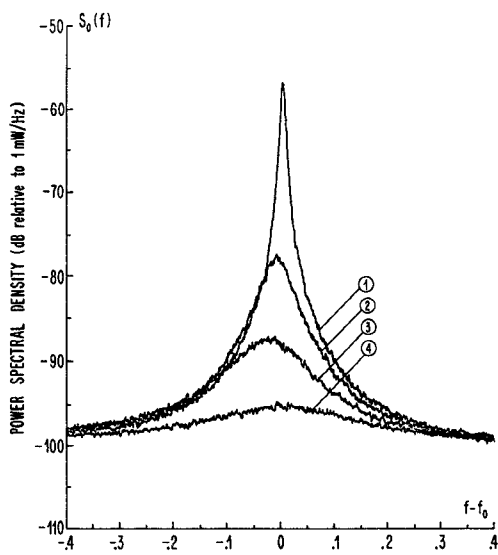
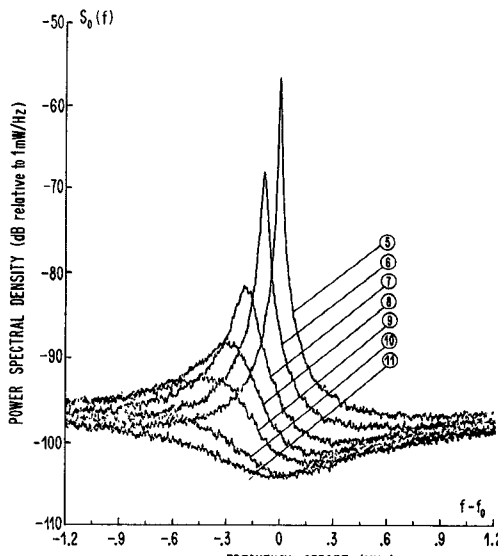


Fig. 3. Calibration curves of the loop gain and phase shift for (a) various attenuator settings (a), (b) various phase shifter settings (p), and (c) various output powers (P_0).

symmetrical around the resonant frequency of the cavity (6.835 GHz). The height increases rapidly with the loop gain while the noise floor stays at the same level. If the loop gain is set to a value higher than the maximum one used here, the system starts to oscillate. The output power grows until the gain of the amplifier compresses (see Fig. 3(c)) and the total loop gain equals the losses in the cavity and its coupling elements. The frequency of the maximum value varies slightly because the total phase shift of the



(a)

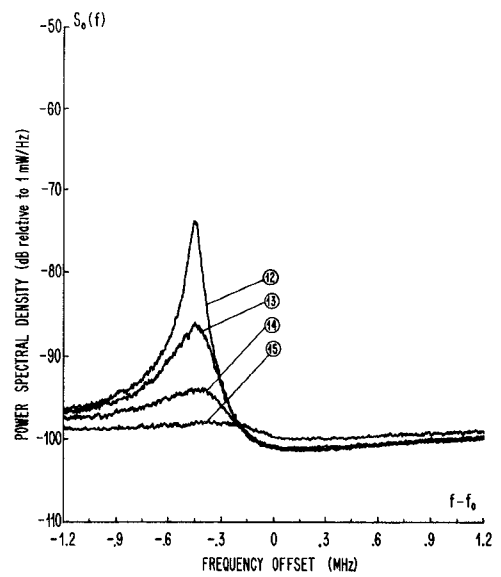


(b)

Fig. 4. Power spectral density of thermal noise delivered to a load as a function of frequency offset from the cavity resonant frequency f_0 for (a) various attenuator settings: (1) $a = 2.79$, (2) $a = 2.70$, (3) $a = 2.55$, (4) $a = 2.30$, and a constant phase shifter setting: $p = 5.98$ ($\psi = 0$); (b) various phase shifter settings: (5) $p = 5.98$, (6) $p = 5.70$, (7) $p = 5.40$, (8) $p = 5.10$, (9) $p = 4.80$, (10) $p = 4.20$, (11) $p = 3.60$, and a constant attenuator setting: $a = 2.79$; (c) various attenuator settings: (12) $a = 4.50$, (13) $a = 3.50$, (14) $a = 3.00$, (15) $a = 2.30$, and a constant phase shifter setting: $p = 4.80$ ($\psi = \pi/2$).

loop changes with the attenuator setting as shown in Fig. 3(c).

If the attenuator setting is maintained at a fixed value ($a = 2.79$) and the phase shifter setting is varied, the noise-power spectral density varies as shown in Fig. 4(b). In this figure, the loop phase shift varies from $\approx 0^\circ$ to 180° . At $\psi \approx 0^\circ$ ($p = 5.98$), curve 5 corresponds to curve 1 of Fig. 4(a). For $\psi \approx 180^\circ$ ($p = 3.60$), the noise spectral distribution is reduced symmetrically around the resonant frequency ($f_0 = 6.835$ GHz) of the cavity. For the other



(c)

TABLE I
MICROWAVE CAVITY AND FEEDBACK LOOP PARAMETERS

k = Boltzmann constant:	1.381×10^{-23} J/K
β_1 = input coupling coefficient:	0.25
β_2 = output coupling coefficient:	0.25
Q_0 = unloaded cavity quality factor:	25000
f_0 = cavity resonant frequency:	6.835 GHz
G_a = amplifier voltage gain:	17.48 (24.8dB)
G_s = power splitter voltage gain:	0.668 (-3.5dB)
G_R = receiver voltage gain:	573.5 (55.2dB)
T_a = amplifier equivalent noise temperature:	190K
T_R = receiver equivalent noise temperature:	254K
θ_1 = thermodynamic temperature of isolator 1:	290K
θ_2 = thermodynamic temperature of isolator 2:	290K
θ_c = thermodynamic temperature of the cavity:	290K

phase settings, the distributions are not symmetrical and a hump appears at a frequency offset from f_0 .

When the phase shifter setting is maintained at a value close to $\pi/2$ while the loop gain is varied, the noise spectral distribution changes, as shown in Fig. 4(c). A hump appears at a frequency which differs from the free resonant frequency of the cavity.

It was observed that oscillation condition can be reached for a phase shifter setting different from $p = 5.98$ ($\psi \approx 0^\circ$) if the loop gain is sufficiently high.

C. Theoretical Calculations

A theoretical evaluation of (7) has been performed for various parameter settings of the system studied. The values of the fixed parameters are given in Table I.

For each experimental curve of Fig. 4(a)–(c), we need to evaluate the “real” gain and phase of the loop. Curve 1 of Fig. 4(a) has been taken at a setting which gives the most

symmetrical spectrum we could get; the loop phase shift is then 0° . The associated loop gain is adjusted to give the same peak level as curve 1 of Fig. 4(a) and is found to be 9.45 dB. From the calibration curves, we get $G = 12$ dB and $\psi = 37.5^\circ$. The loop gain and phase for the other curves will then be obtained straightforwardly by taking off 2.55 dB from the "calibrated" gain and 37.5° from the phase. These represent constant losses and phase shifts associated with the cavity coupling elements. The resulting values, and the corresponding plots are shown in Fig. 5(a)–(c). For each curve, we indicate the value of G and ψ deduced from the loop parameter settings and the calibration curves of Fig. 3(a)–(c).

We observe a good agreement between the theoretical calculations and experimental data and notice that, even if the curves are not taken at "round" values of loop gain and phase, the calibration used allows an effective evaluation of these variables.

We have shown through a thorough experimental study that (7) properly expresses the power spectral density of the thermal noise generated in a microwave system consisting of a cavity and a feedback loop to enhance the cavity Q factor. This relation and its theoretical background can then be used with confidence to evaluate fundamental processes related to thermal noise of similar microwave systems.

Figs. 6 and 7 give the variation of the "apparent" cavity Q and the cavity "apparent" resonant frequency as functions of loop gain and phase. In the case of Fig. 6(a) and (b), the phase is quasiconstant (approx. 0°) while the gain is changed. The exact values of gain and phase for each setting are obtained through the use of calibration curves given in Fig. 3(a)–(c) and are used in numerical evaluation of (8) and (9). The results obtained through calculation are represented by a circle and the measured data by a cross. In Fig. 7(a) and (b), the gain is considered quasiconstant (approx. 7 dB) while the phase is shifted. Again, the results of the calculation are shown with circles and the results of measurement are crosses. These four figures indicate that (8) and (9) are well verified through the experiment. We now look at some aspects of the frequency stability characterization of this system operated as a cavity-oscillator.

III. FREQUENCY STABILITY

The RF spectrum $S_{RF}(f)$ of a highly stable oscillator is, under certain conditions, simply related to the spectral density of its phase fluctuations $S_\phi(f)$ by the relation [4]

$$S_{RF}(f) = \frac{P}{2} [\delta(f - f_0) + S_\phi(f - f_0)] \quad (10)$$

where P is the output power and $\delta(f - f_0)$ is the Dirac delta function. $S_\phi(f)$ corresponds to the baseband noise and is sometimes mentioned in terms of $\mathcal{L}(f)$ [5], [6]. We see from (10) that the knowledge of $S_\phi(f)$ allows a prediction of some part of the RF spectrum of a precision oscillator.

The short-term frequency stability measurement in the frequency domain is defined in terms of the spectral den-

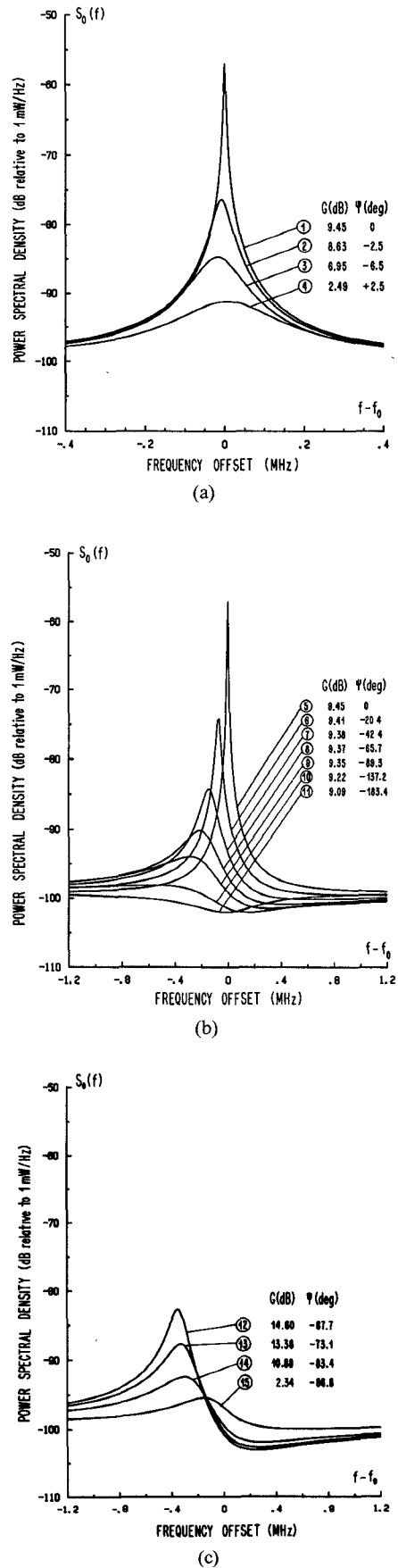
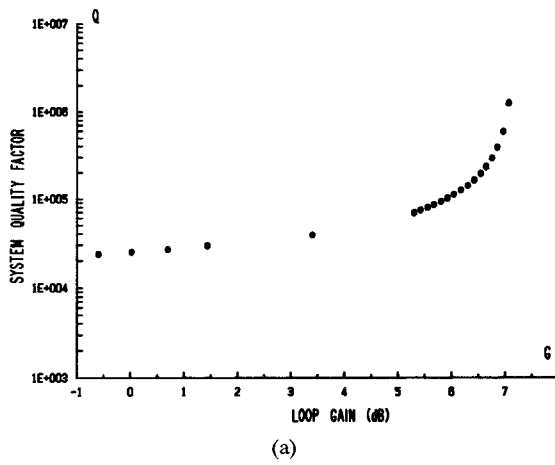
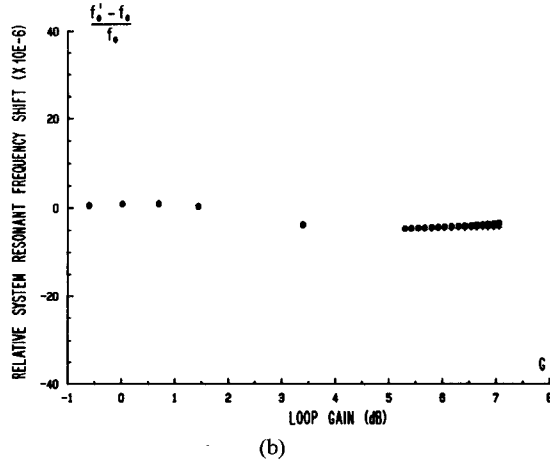


Fig. 5. Theoretical evaluation of the power spectral density of the thermal noise for (a) parameter settings equivalent to Fig. 4(a), (b) parameter settings equivalent to Fig. 4(b), and (c) parameter settings equivalent to Fig. 4(c).



(a)



(b)

Fig. 6. Modified cavity Q and cavity resonant frequency as functions of the loop gain when the total phase shift is quasiconstant: experimental data (+), theoretical calculation (○). (a) Quality factor and (b) relative resonant frequency shift.

sity of the phase fluctuations or in terms of the spectral density of the relative frequency fluctuations $S_y(f)$ [7]. The two densities are related in usual cases by

$$S_y(f) = \frac{f^2}{f_0^2} S_\phi(f). \quad (11)$$

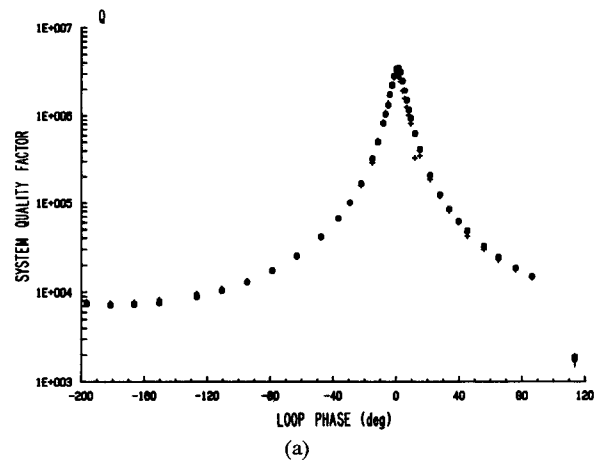
Measurement of the short-term frequency stability in the time domain is defined by the two-sample variance of the mean fractional frequency fluctuations over an averaging time τ , $\sigma_y^2(\tau)$, (often called Allan variance) [7]. This variance is linked to the spectral density $S_y(f)$ by the relation

$$\sigma^2(\tau) = 2 \int_0^\infty S_y(f) \frac{\sin 4\pi f \tau}{(\pi f \tau)^2} \left(\frac{1}{1 + (f/f_h)^2} \right) df \quad (12)$$

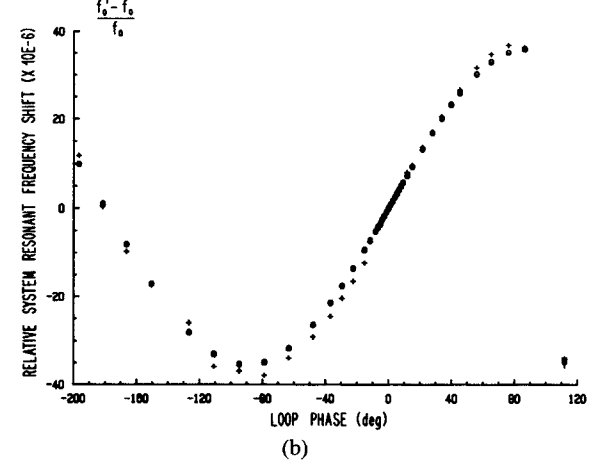
where the spectrum of the fluctuations are supposedly limited by a first-order low-pass filter of cutoff frequency f_h .

A. Time-Domain Measurement

We have measured the frequency stability of a microwave cavity-oscillator as considered in the previous section by beating its output signal to the signal of a reference oscillator and analyzing the beat signal generated in an



(a)



(b)

Fig. 7. Modified cavity Q and cavity resonant frequency as functions of the loop total phase shift when the gain is quasiconstant; experimental data (+), theoretical calculation (○). (a) Quality factor and (b) relative resonant frequency shift.

AM heterodyne receiver (see Fig. 8). This approach allows a transfer of the absolute microwave frequency instabilities to a much lower beat frequency, thus increasing the relative value of these instabilities, and is currently used in atomic oscillator characterization [8]. This measurement system is independent of the local oscillator performance since this oscillator produces only a translation of the AM information to the IF signal. In the measurements presented here, the reference oscillator is a rubidium maser oscillator [9] but a similar cavity-oscillator gives the same information also. The beats signal frequency was set at approximately 150 kHz and filtered through a bandpass filter of 200-kHz bandwidth.

The time-domain measurement is done directly with a period counter feeding a computer. The results obtained are shown in Fig. 9(a) as the two-sample standard deviation, for various averaging times. This curve shows that the two-sample variance can be estimated to

$$\sigma^2(\tau) \approx 3 \times 10^{-18} \tau^\alpha \quad \text{for } 10^{-4} \text{ s} \leq \tau \leq 1 \text{ s} \quad (13a)$$

and

$$\sigma^2(\tau) \approx 3 \times 10^{-20} \tau^{+2} \quad \text{for } 1 \text{ s} \leq \tau \leq 100 \text{ s.} \quad (13b)$$

The first type of frequency instabilities (τ^α) is referred to

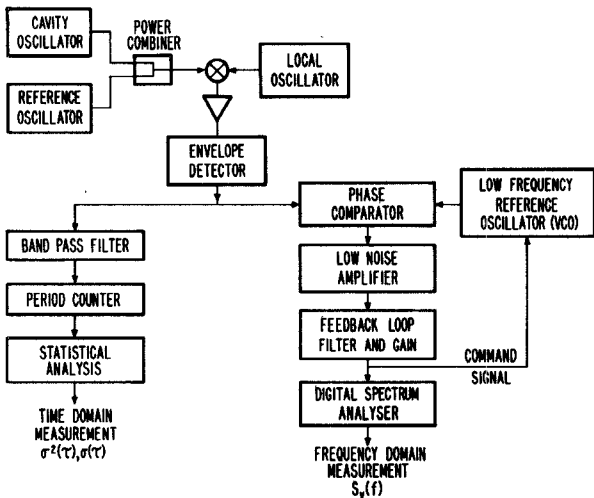


Fig. 8. Experimental setup used to measure the short-term frequency stability of a microwave oscillator both in the time domain and in the frequency domain.

as flicker of frequency noise and is likely to be associated with noise generated in the feedback loop FET amplifier [11]. The second term (τ^{+2}) is related to frequency drift and comes eventually from cavity temperature drift during the measurement time.

B. Frequency-Domain Measurement

We have measured the frequency stability of the microwave cavity-oscillator in the frequency domain through the method of tight phase locking of a reference oscillator [10]. A highly stable low-frequency synthesizer is phase locked to the beat signal over a wide frequency loop bandwidth (see right part of Fig. 8). The command signal is then proportional to the beat signal frequency fluctuations which are those of the microwave cavity-oscillator and its spectral density is measured directly with a digital spectrum analyzer (EMR-1510).

The results obtained for the frequency range of 1–256 Hz are given in Fig. 9(b). We observe clearly a flicker of frequency noise expressed as

$$S_y(f) = 4 \times 10^{-18} f^{-1} \quad \text{for } 6 \text{ Hz} \leq f \leq 256 \text{ Hz.} \quad (14)$$

If we use the translation relation defined in (12), we find that this contribution should give, for a time-domain measurement, an Allan variance of $2.7 \times 10^{-18} \tau^{\circ}$, which effectively confirms the result given in the previous section (see (13a)).

The frequency-domain measurement indicates that the phase-noise spectral density evaluated through (11) should be

$$S_\phi(f) = 2 \times 10^2 f^{-3} \quad \text{for } 6 \text{ Hz} \leq f \leq 256 \text{ Hz} \quad (15)$$

so the RF spectrum of this oscillator should have a portion close to carrier equal to $\frac{1}{2} S_\phi(f)$ (see (10)). As already mentioned, this behavior is encountered in the study of microwave feedback oscillators using FET amplifiers [11] and is likely to be generated in the amplifier itself.

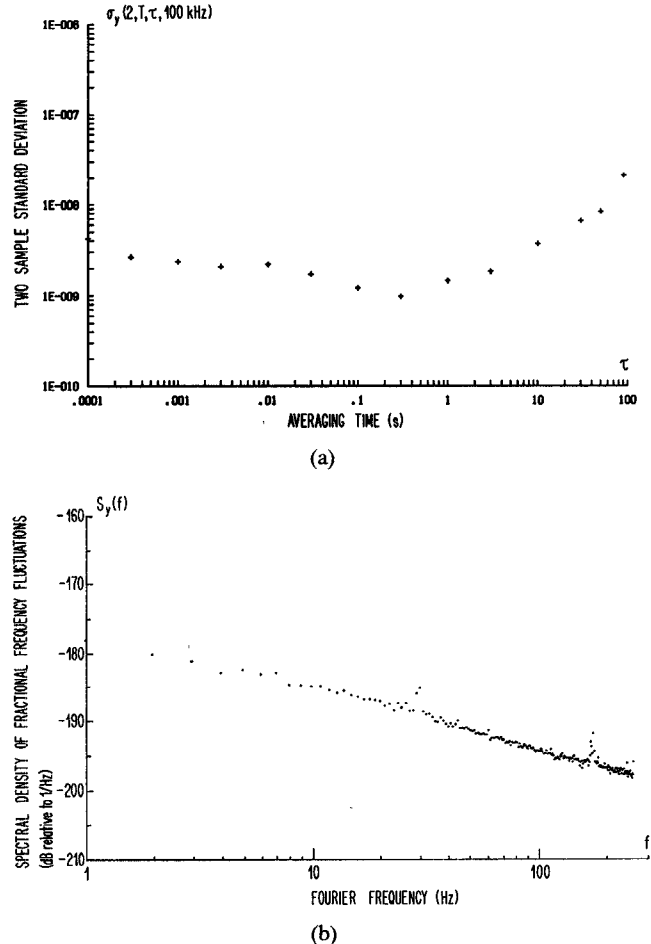


Fig. 9. Measurement of short-term frequency stability of a cavity-oscillator. (a) Time-domain measurement: Allan variance. (b) Frequency-domain measurement: Spectral density of the fractional frequency fluctuations.

IV. CONCLUSION AND DISCUSSION

We have established a formalism that allows the computation of the thermal noise generated in a system consisting of a microwave cavity equipped with an external feedback loop. We have proved the validity of the model by a thorough experimental study, so the effect of any parameter changes can be predicted with accuracy. This approach can be applied to other types of feedback oscillators.

A measurement setup used to characterize the short-term frequency stability of atomic frequency standards has been adapted to study the system operated as a microwave cavity-oscillator. The frequency stability exhibits a τ° dependency for a time-domain measurement or a flicker of frequency noise, f^{-1} dependency, for the spectral density of the fractional frequency fluctuations (FM noise). More measurements are needed in order to fully characterize the behavior of this system as a microwave oscillator.

REFERENCES

- [1] C. Audoin, "Le maser à hydrogène en régime transitoire," *Rev. Phys. Appl.*, vol. 2, pp. 309–320, 1967.
- [2] H. T. M. Wang, "An oscillating compact hydrogen maser," in *Proc. 34th Ann. Symp. on Frequency Control*, 1980, pp. 364–369.
- [3] M. Tétu, P. Tremblay, P. Lesage, and P. Petit, "Experimental study of the frequency stability of a maser oscillator operated with an

external feedback loop," *IEEE Trans. Instrum. Meas.*, vol. IM-32, pp. 410-413, 1983.

[4] J. Rutman, "Characterization of phase and frequency instabilities in precision frequency sources: Fifteen years of progress," *Proc. IEEE*, vol. 66, pp. 1048-1075, Sept. 1978.

[5] J. H. Shoaf, D. Halford, and A. S. Risley, "Frequency stability specifications and measurement: High frequency and microwave signals," *NBS Tech. Note 632*, Jan. 1973.

[6] A. L. Lance, W. D. Seal, F. G. Mendoza, and N. W. Hudson, "Automating phase noise measurements in the frequency domain," in *Proc. 31st Ann. Symp. Frequency Contr.*, (Atlantic City, NJ), 1977, pp. 347-358.

[7] J. A. Barnes *et al.*, "Characterization of frequency stability," *IEEE Trans. Instrum. Meas.*, vol. IM-20, pp. 105-120, 1971.

[8] M. Tétu, R. Brousseau, and J. Vanier, "Frequency-domain measurement of the frequency stability of a maser oscillator," *IEEE Trans. Instrum. Meas.*, vol. IM-29, pp. 94-97, 1980.

[9] M. Tétu, G. Busca, and J. Vanier, "Short-term frequency stability of the Rb⁸⁷ maser," *IEEE Trans. Instrum. Meas.*, vol. IM-22, pp. 250-257, 1973.

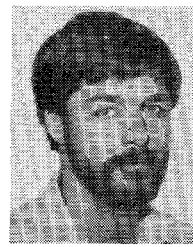
[10] B. E. Blair, Ed., *Time and Frequency: Theory and Fundamentals*. Washington, DC: U.S. Dept. Commerce, NBS Mon. 140, 1974, ch. 8.

[11] R. A. Pucel and J. Curtis, "Near-carrier noise in FET oscillators," in *1983 IEEE MTT-S Int. Microwave Symp. Dig.*, pp. 282-284.



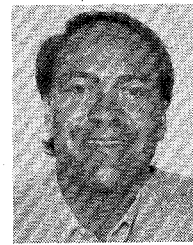
Pierre Tremblay (S'78) was born in Saint-Joachim, Quebec, Canada, on October 16, 1958. He received the B.Sc.A. and M.Sc. degrees in electrical engineering from Laval University, Quebec, Canada, in 1981 and 1983, respectively. He is presently studying towards the Ph.D. degree at Laval University, where he is working in the area of atomic frequency standards.

+



Alain Michaud (S'79) was born in Murdochville, Quebec, Canada, on December 12, 1958. He received the B.Sc.A. degree in electrical engineering from Laval University, Quebec, Canada, in 1982, and is presently studying towards the M.Sc. degree at the same institution. His research interests are simulation of phase-locked loops and their application to atomic frequency standards.

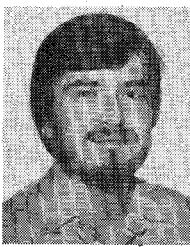
+



Michel Tétu (M'74-SM'83) was born in Quebec, P.Q., Canada, on May 31, 1944. He received the B.Sc. and M.Sc. degrees in physics in 1967 and 1971, respectively, and the D.Sc. degree in electrical engineering from Laval University, Quebec, in 1972.

In 1973 and 1974, he worked as a Research Associate at the Center for Astrophysics, Cambridge, MA, on the Smithsonian Astrophysical Observatory Red Shift Program. Since 1974, he has been a Professor at the Department of Electrical Engineering, Laval University. His major research is concerned with the development and the use of atomic frequency standards.

Dr. Tétu is a member of the American Physical Society, the Canadian Association of Physicists, and the Optical Society of America.



Bernard Villeneuve (S'78) was born in Beauport, Quebec, Canada, on May 9, 1959. He received the B.Sc.A. and M.Sc. degrees in electrical engineering from Laval University, Quebec, Canada, in 1982 and 1984, respectively. He is presently working towards the Ph.D. degree at the same institution in the area of microwave oscillator noise.
